On Solving TM_{0n} Modal Excitation in a Ka-Band Overmoded Circular Waveguide by the Conservation of Complex Power Technique

Feng Lan, Xi Gao, and Zong-Jun Shi

***Abstract*—To measure the radiation properties of relativistic diffraction generator (RDG) in Ka-band, a TM_{0n} modal excitation model is established, which consists of an overmoded circular waveguide and a coaxial line feeding probe. Using the transverse E-field mode matching and the conservation of complex power technique (CCPT), we deduce the scattering matrix at coaxial line to coaxial line and coaxial line to circular waveguide junctions. Then using the overall cascaded junction scattering matrix, the numerical results for the reflection coefficient of the coaxial line and the power distribution of TM_{0n} multi-modal are presented. The numerical results are in agreement with HFSS simulation results and experimental results. The analysis shows that by choosing the appropriate position of coaxial line probe, the power proportion of the device operating mode excited in circular waveguide could be the largest.**

***Index Terms*—Coaxial excitation, conservation of complex power technique, overmoded waveguide, relativistic diffraction generator.**

1. Introduction

In high power millimeter wave radiation source which is driven by relativistic electronic beam, overmoded circular waveguide is chosen as output high frequency system usually for raising device power capacity[1],[2]. For ascertaining the radiation pattern of the conical antenna with overmoded circular waveguide, the TM_{0n} symmetrical multi-modal excitation of a coaxial line probe-to-circular waveguide is introduced. The probe is placed at the waveguide axes to excite symmetrical TM_{0n} modes, but the position of probe tine affects the transverse efficiency of TEM mode to TM_{0n}[3] modes. For the purpose of discussing the transverse efficiency of TEM to TM_{0n} in Ka-band overmoded circular waveguide, a rigorous full-wave solution by means of the conservation of complex power technique (CCPT) and HFSS simulations are given. The numerical results obtained by CCPT and HFSS simulation for a overmoded circular waveguide fed by an coaxial probe and a 50 Ω semirigid coaxial cable show quite good agreement.

Manuscript received January 16, 2008; revised February 21, 2009. This work was supported by the National Natural Science Foundation of China under Grant No. 60571020.

The authors are with School of Physical Electronics, University of Electronic Science and Technology of China, Chengdu, 610054, China (e-mail: lanf998@tom.com, gao_xi76@163.com, shizongjun@163.com).

2. Deduction of the Overall Scattering Matrix by the E-Field Mode Matching and CCPT

Fig. 1 illustrates the geometry of the forepart of the output window, which includes three waveguides: the small coaxial line for $z<0$ (Guide 1), the larger coaxial line for $0<z<l$ (Guide 2), and the overmoded circular guide for $l<z<L$ (Guide 3). The stimulant signal is fed-in by TEM mode from Guide 1. We assume that the circular waveguide is long enough, only TM_{0n} modes can be excited for the circular rotary symmetry. In particular, we are concerned with the scattering of a TEM mode incident from the small coaxial line and the coaxial probe tine position where the dominant mode is TM_{04} matching with high frequency system.

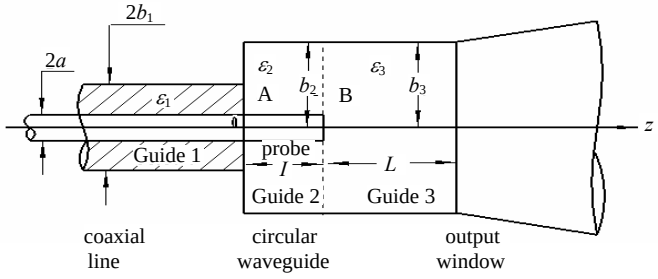

Fig. 1. An overmoded circular waveguide with an output conical antenna fed by a coaxial line probe for TM_{0n} modes excitation.

Instead of mode matching the tangential magnetic field in the classical solution[4],[5], the CCPT is invoked and leads to an expression for the junction's input admittance matrix as seen from the smaller guide to obtain scattering matrices. At each junction (A and B), the scattering matrices $\mathbf{S}^{A}$ and $\mathbf{S}^{B}$ for the modal amplitudes of the TM_{0n} modes excited by a TEM mode incident from Guide 1 are obtained by the transverse E-field mode matching and the CCPT. First we

deduced the analytical expressions of the E-filed mode matching matrices $\mathbf{M}^{\mathrm{A}}$ and $\mathbf{M}^{\mathrm{B}}$ which are necessary to deduce $\mathbf{S}^{\mathrm{A}}$ and $\mathbf{S}^{\mathrm{B}}$.

1) M^{A} (at the coaxial-coaxial junction A):

The *nm*th element of $\mathbf{M}^{\mathrm{A}}$ for TM_{0n} modes only in two coaxial line is:

$$M_{nm}^{\mathrm{A}} = 2\pi \frac{\beta_{2n}\beta_{1m}}{\beta_{2n}^2-\beta_{1m}^2}\Big[\beta_{2n}\rho Z_1(\beta_{1m}\rho)Z_2(\beta_{2n}\rho) - \beta_{1m}\rho Z_1(\beta_{2n}\rho)Z_2(\beta_{1m}\rho)\Big]\Big|_a^{b_1} \tag{1}$$

where for n=1, 2, ⋯, m=1, 2⋯, i=1, 2, and q=1,2⋯. β_{iq} satisfies the transcendental equations:

$$J_0(\beta_{iq}b_i)N_0(\beta_{iq}a) - N_0(\beta_{iq}b_i)J_0(\beta_{iq}a) = 0 \tag{2}$$

and for j=1, 2:

$$Z_j(\beta_{iq}\rho) = \frac{\sqrt{\pi}}{2}\frac{J_j(\beta_{iq}\rho)N_0(\beta_{iq}a) - N_j(\beta_{iq}\rho)J_0(\beta_{iq}a)}{\left[\dfrac{J_0^2(\beta_{iq}a)}{J_0^2(\beta_{iq}b_i)}-1\right]^{1/2}}. \tag{3}$$

For the case of TEM mode incident from one side at junction A, if $N_{i0} = \left[2\pi\ln\left(b_i/a\right)\right]^{-1/2}$, then

$$M_{00}^{\mathrm{A}} = 2\pi N_{10}N_{20}\ln(b_1/a) \tag{4}$$

$$M_{n0}^{\mathrm{A}} = 2\pi N_{10}\left[Z_0(\beta_{2n}\rho)\Big|_a^{b_1}\right] \tag{5}$$

$$M_{0m}^{\mathrm{A}} = 0. \tag{6}$$

2) $\mathbf{M}^{\mathrm{B}}$ **(at the coaxial-circular waveguide junction** B**):**

The *nm*th element of $\mathbf{M}^{\mathrm{B}}$ for TM_{0n} modes only in both sides at junction B is

$$M_{nm}^{\mathrm{B}} = \frac{2\sqrt{\pi}\beta_{2m}[\beta_{3n}\rho Z_1(\beta_{2m}\rho)J_2(\beta_{3n}\rho)}{b_3J_1(\beta_{3n}b_3)(\beta_{3n}^2-\beta_{2m}^2)} - \beta_{2m}\rho\, J_1(\beta_{3n}\rho)Z_2(\beta_{2m}\rho)]\Big|_a^{b_2} \tag{7}$$

where $\beta_{3n}b_3$ is the nth root of $J_0(x)$, for j=1, 2 and $m\neq 0$.

$$Z_j(x) = \frac{\sqrt{\pi}}{2}\frac{J_j(x)N_0(\beta_{iq}a) - N_j(x)J_0(\beta_{iq}a)}{\left[\dfrac{J_0^2(\beta_{iq}a)}{J_0^2(\beta_{iq}b_i)}-1\right]^{1/2}}. \tag{8}$$

If m=0, $n\neq 0$

$$M_{n0}^{\mathrm{B}} = \frac{2\sqrt{\pi}N_{20}}{\beta_{3n}b_3J_1(\beta_{3n}b_3)}\left[J_0(\beta_{3n}b_2) - J_0(\beta_{3n}a)\right]. \tag{9}$$

3) $\mathbf{S}^{\mathrm{A}}$ **and** $\mathbf{S}^{\mathrm{B}}$ **(scattering matrices at junction A and B):**

The CCPT and the E-filed mode matching matrices $\mathbf{M}^{\mathrm{A}}$, $\mathbf{M}^{\mathrm{B}}$ are used to obtain the junction's input admittance matrices $\mathbf{Y}_{\mathrm{L1}}$ and $\mathbf{Y}_{\mathrm{L2}}$ and scattering matrices $\mathbf{S}^{\mathrm{A}}$ and $\mathbf{S}^{\mathrm{B}}$.

$$\mathbf{Y}_{\mathrm{L1}} = (\mathbf{M}^{\mathrm{A}})^T\mathbf{Y}_2\mathbf{M}^{\mathrm{A}} \tag{10}$$

$$\mathbf{S}_{11}^{\mathrm{A}} = (\mathbf{Y}_1+\mathbf{Y}_{\mathrm{L1}})^{-1}(\mathbf{Y}_1-\mathbf{Y}_{\mathrm{L1}}) \tag{11}$$

$$\mathbf{S}_{21}^{\mathrm{A}} = \mathbf{M}^{\mathrm{A}}(\mathbf{S}_{11}^{\mathrm{A}}+\mathbf{I}) \tag{12}$$

$$\mathbf{S}_{12}^{\mathrm{A}} = 2(\mathbf{Y}_1+\mathbf{Y}_{\mathrm{L1}})^{-1}\mathbf{M}^T\mathbf{Y}_2 \tag{13}$$

$$\mathbf{S}_{22}^{\mathrm{A}} = \mathbf{M}^{\mathrm{A}}\mathbf{S}_{12}^{\mathrm{A}} - \mathbf{I} \tag{14}$$

$$\mathbf{Y}_{\mathrm{L2}} = 2(\mathbf{M}^{\mathrm{B}})^T\mathbf{Y}_3\mathbf{M}^{\mathrm{B}} \tag{15}$$

$$\mathbf{S}_{22}^{\mathrm{B}} = (\mathbf{Y}_2+\mathbf{Y}_{\mathrm{L2}})^{-1}(\mathbf{Y}_2-\mathbf{Y}_{\mathrm{L2}}) \tag{16}$$

$$\mathbf{S}_{32}^{\mathrm{B}} = \mathbf{M}^{\mathrm{B}}(\mathbf{S}_{22}^{\mathrm{B}}+\mathbf{I}) \tag{17}$$

$$\mathbf{S}_{23}^{\mathrm{B}} = 2(\mathbf{Y}_2+\mathbf{Y}_{\mathrm{L2}})^{-1}\mathbf{M}^T\mathbf{Y}_3 \tag{18}$$

$$\mathbf{S}_{33}^{\mathrm{B}} = \mathbf{M}^{\mathrm{B}}\mathbf{S}_{23}^{\mathrm{B}} - \mathbf{I} \tag{19}$$

where $\mathbf{Y}_{\mathrm{L1}}$ and $\mathbf{Y}_{\mathrm{L2}}$ are the input admittance matrices of A and B junction networks, $\mathbf{Y}_1$ and $\mathbf{Y}_2$ are the modal admittances of Guide 1 and Guide 2 respectively. $\mathbf{I}$ is the unit matrix.

Scatter matrix of the overall cascaded junction[6]:

$$\mathbf{S}_{11}^{\mathrm{r}} = \mathbf{S}_{11}^{\mathrm{A}} + \mathbf{S}_{12}^{\mathrm{A}}\mathbf{L}_2\mathbf{S}_{22}^{\mathrm{B}}\mathbf{G}_1^{-1}\mathbf{L}_2\mathbf{S}_{21}^{\mathrm{A}} \tag{20}$$

$$\mathbf{S}_{31}^{\mathrm{t}} = \mathbf{S}_{32}^{\mathrm{B}}\mathbf{G}_1^{-1}\mathbf{L}_2\mathbf{S}_{21}^{\mathrm{A}} \tag{21}$$

$$\mathbf{G}_1^{-1} = \mathbf{I} - \mathbf{L}_2\mathbf{S}_{22}^{\mathrm{A}}\mathbf{L}_2\mathbf{S}_{22}^{\mathrm{B}} \tag{22}$$

where $\mathbf{S}_{11}^{\mathrm{r}}$ is the backscattered matrix which relates the TEM incident and the TM_{0n} modes excited by TEM in Guide 1. $\mathbf{S}_{31}^{\mathrm{t}}$ is the transmission matrix which relates the TEM incident and the TM_{0n} modes excited by TEM from Guide 1 to Guide 3. $\mathbf{L}_2$ is the diagonal line matrix, whose diagonal element is:

$$L_{2,nn} = e^{-\gamma_{2n}l} \tag{23}$$

where γ_{2n} is the propagation constant of the TM_{0n}th mode in Guide 2, and l is the length of the probe tine going through Guide 2.

The TEM reflection coefficient in Guide 1 can be obtained by the backscattered matrix $\mathbf{S}_{11}^{\mathrm{r}}$, so:

$$\Gamma = S_{11,00}^{\mathrm{r}} \tag{24}$$

The normalized power of the backscattered modes in Guide 1 and the transmission modes in Guide 3 compared with incident mode TEM is:

$$P_{1,mm} = |S_{11}^{\mathrm{r}}|^2\frac{Y_{1,m}^*}{Y_{1,0}^*} \tag{25}$$

$$P_{3,nn} = |S_{31}^{\mathrm{t}}|^2\frac{Y_{3,n}^*}{Y_{1,0}^*} \tag{26}$$

where $Y_{i,n}$ is the nth modal characteristic admittance in Guide i.

Based on CCPT, it comes into existence:

$$\mathrm{R_e}\left[\sum_m P_{1,m} + \sum_n P_{3,n}\right] = 1 \tag{27}$$

3. Numerical and Simulation Results

The model parameters we concerned are: $\varepsilon_1=2.2\varepsilon_0$, $\varepsilon_2=\varepsilon_3=\varepsilon_0$, a=0.3 mm, b_1=1.05 mm, $b_2=b_3$=19.8 mm, $l+L$= 40 mm. In order to avoid the relative convergence problem, we typically used $N_2^{\mathrm{A}}/N_1^{\mathrm{A}} \geq b_2/b_1$ at junction A, $N_2^{\mathrm{B}}=N_3^{\mathrm{B}} < N_2^{\mathrm{A}}$ at junction B (N_2^{B} denotes mode number in Guide 2, N_3^{B} denotes mode number in Guide 3).

Table 1: Numerical verification of power conservation for the case of f=31 GHz, l / λ=0.3

Mode number	P_{total}
N_1^{A}=3 N_2^{A}=50 $N_2^{\mathrm{B}}=N_3^{\mathrm{B}}$=20	1.1353
N_1^{A}=3 N_2^{A}=50 $N_2^{\mathrm{B}}=N_3^{\mathrm{B}}$=25	1.1378
N_1^{A}=5 N_2^{A}=100 $N_2^{\mathrm{B}}=N_3^{\mathrm{B}}$=20	0.9999
N_1^{A}=5 N_2^{A}=100 $N_2^{\mathrm{B}}=N_3^{\mathrm{B}}$=25	0.9999

The results shown in Table 1 indicate that the accuracy is much better than 0.1% when N_1^{A}=5, N_2^{A}=100, $N_2^{\mathrm{B}}= N_3^{\mathrm{B}}$=20. Typically, we used 5 modes in Guide 1 (N_1^{A}=5) and 100 modes in Guide 2 (N_2^{A}=100) to compute the scattering matrix $\mathbf{S}_{11}^{\mathrm{A}}$ in (11); moreover, in all cases $N_2^{\mathrm{A}}/N_1^{\mathrm{A}} \geq b_2/b_1$, to avoid relative convergence. To calculate $\mathbf{S}_{11}^{\mathrm{A}}$, one needs to invert a matrix of size 5×5 only. Moreover, if only the TM_{01}, TM_{02}, TM_{03}, TM_{04} mode can propagate, then most of the N_2^{A}=100 mode fields transmitted into Guide 2 will have negligible amplitude when they reach junction B. As a result, in our computations involving $\mathbf{S}^{\mathrm{B}}$, we typically set $N_2^{\mathrm{B}}= N_3^{\mathrm{B}}$=20.

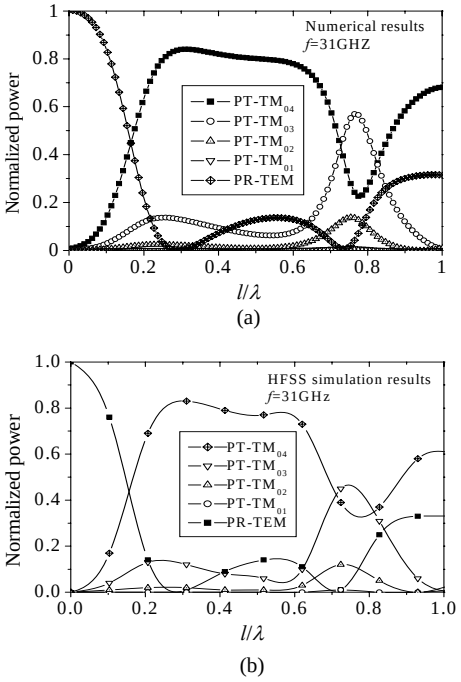

Fig. 2. Numerical and HFSS simulation results of normalized power of TM_{0n} transmission modes excited by TEM and TEM reflection in the circular waveguide as a function probe length l/λ at f=31 GHz: (a) numerical results and (b) HFSS results.

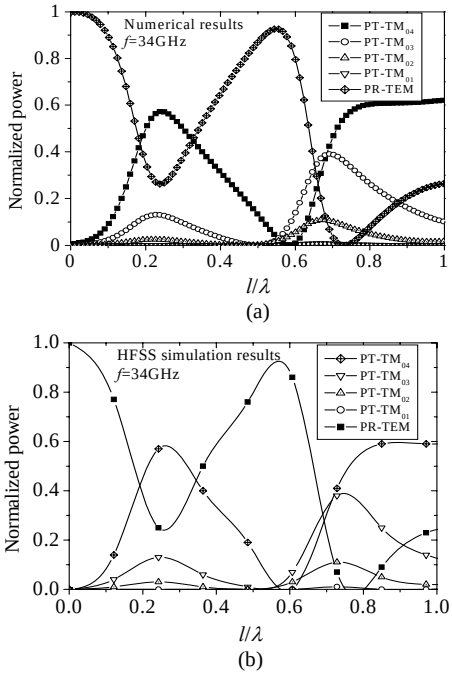

Fig. 3. Numerical and HFSS simulation results of normalized power of TM_{0n} transmission modes excited by TEM and TEM reflection in the circular waveguide as a function probe length l/λ at f=34 GHz: (a) numerical results and (b)HFSS results.

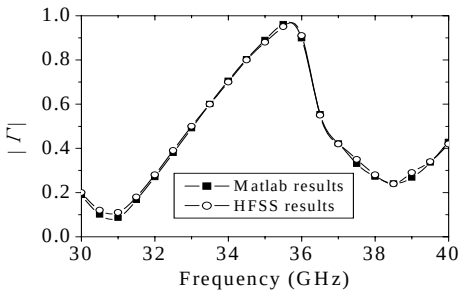

Fig. 4. Numerical and HFSS simulation results of TEM reflection coefficient $|\Gamma|$ versus frequency for l=3 mm.

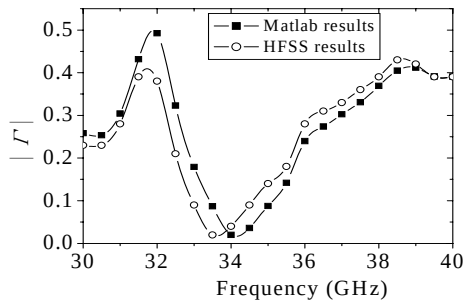

Fig. 5. Numerical and HFSS simulation results of TEM reflection coefficient $|\Gamma|$ versus frequency l=6.4 mm.

The numerical results and simulation results show quite good coincidence. In Fig. 2 and Fig. 3, we compute the normalized power of TM_{0n} transmission excited by TEM

and TEM reflection in the circular waveguide as a function probe length l/λ at f=31 GHz and 34 GHz. When f=31 GHz, TEM reflection power is lowest at l/λ≈0.3 and l/λ≈0.73. That corresponds with the highest transmission power from coaxial line to circular waveguide. When f=34 GHz, TEM reflection power is lowest at l/λ≈0.25 and l/λ≈0.73. That corresponds with the highest transmission power from coaxial line to circular waveguide. Fig. 4 and Fig. 5 provide the sweeping frequency curves of TEM reflection coefficient $|\Gamma|$ by numerical calculation and HFSS simulation. The TEM reflection coefficient $|\Gamma|$ is lowest at f=31 GHz and 34 GHz when l=3 mm and 6.4 mm accord with the power distribution curve. At f=31 GHz and 34 GHz, TM_{01}, TM_{02}, TM_{03}, TM_{04} can be transmitted in the overmoded circular waveguide, and the highest transmission mode takes advantage in the power distribution mostly.

4. Comparison of Experimental and Simulation Results for TEM Reflection Coefficient

The RDG output window is connected with an overmoded circular waveguide fed by a coaxial probe, then the additional simulation results and experimental results of coaxial line reflection coefficient S_{11} for the case of f=30~40 GHz, l=5.7 mm are given in Fig. 6. The lowest reflection frequency is around 37 GHz. Their coherence is reasonably good except some tiny differences, for cable line attenuation in the Agilent8722ES vector network analyzer and imperfection of output horn terminal matching. The analysis of the results demonstrates that our design method is reliable.

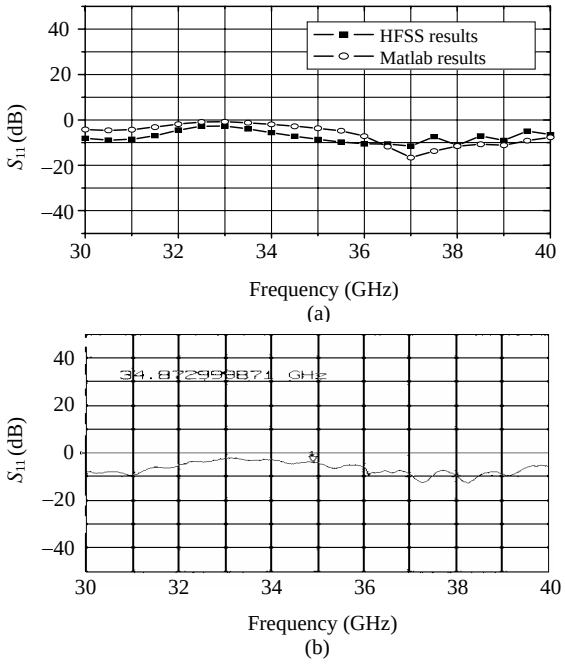

Fig. 6. Numerical and experimental results of TEM reflection coefficient S_{11} versus frequency for l=5.7 mm: (a) simulation results and (b) experimental results.

5. Conclusions

The solution of the conservation of complex power technique (CCPT) for a TM_{0n} modal excitation problem in Ka-band overmoded circular waveguide is given in this paper. Different from the published papers in this field, relationship between mode number and precision of power conservation is discussed in this paper. In addition, the comparison among numerical results, HFSS simulation results and experimental results shows great agreement. The analysis shows that by choosing the appropriate position of coaxial line probe, the power proportion of the highest order mode excited in circular waveguide could be the largest. The CCPT is a reliable method for modal analysis of scattering at waveguide junctions[7]-[11]. Moreover, CCPT spends much less time than HFSS. At current situation, HFSS solution will spend a few hours, however, the CCPT solution spends only about 1 min. By means of CCPT and cascading algorithm to obtain the propagation characteristic of the period corrugation waveguide and antenna will be done in the near future.

References

[1] A. N. Vlasov, A. G. Shkvarunets, and J. C. Rodgers, "Overmoded GW-class surface–wave microwave oscillator," *IEEE Trans. on Plasma Science*, vol. 28, no. 3, pp. 556-560, Jun. 2000.

[2] F. Lan, X. Gao, Z.-J. Shi, Z.-Q. Yang, and Z. Liang, "Measurement of radiation power for Ka-band relativistic diffraction generator," *Journal of University of Electronic Science and Technology of China*, vol. 35, no. 5, pp. 777-779, Oct. 2006 (in Chinese).

[3] C. Yu and G. Wen, "The TM_{0n} multi-modal excitation of a coaxial line probe-to-circular waveguide," *Acta Electonica Sinica*, vol. 26, no. 9, pp. 90-92, Sep. 1998 (in Chinese).

[4] G. G. Gentili, "Properties of TE-TM Mode-Matching Techniques," *IEEE Trans. on Microwave Theory Tech.*, vol. 39, no. 9, pp. 1669-1673, Sep. 1991.

[5] G. V. Eleftheriades, A. S. Omar, L. P. B. Katehi, and G. M. Rebeiz, "Some important properties of waveguide junction generalized scattering matrices in the context of the mode matching technique," *IEEE Trans. on Microwave Theory Tech.*, vol. 42, no. 10, pp. 1896-1903, Oct. 1994.

[6] Y.-H. Liu, H.-F. Li, H. Li, E.-F. Wang, H. Wang, and L. Wang, "Analysis of an open cavity with abrupt transition by mode-matching technique," *Journal of University of Electronic Science and Technology of China*, vol. 35, no. 4, pp. 494-496, Aug. 2006 (in Chinese).

[7] R. H. Macphie and C. R. Ries, "Input impedance of a coaxial line probe feeding a circular waveguide in the TM_{01} mode,"

IEEE Trans. on Microwave Theory Tech., vol. 38, no. 3, pp. 334-337, Mar. 1990.

[8] J. D. Wade and R. H. Macphie, "Conservation of complex power technique for waveguide junctions with finite wall conductivity," *IEEE Trans. on Microwave Theory Tech*., vol. 38, no. 4, pp. 373-378, Apr. 1990.

[9] R. R. Mansour and R. H. Macphie, "Scattering at an n-farcated parallel-plate waveguide junction," *IEEE Trans. on Microwave Theory Tech*., vol. 33, no. 9, pp. 830-835, Sep. 1985.

[10] E. M. Sich and R. H. Macphie, "The conservation of complex power technique and E-plane step-diaphragm junction discontinuities," *IEEE Trans. on Microwave Theory Tech*., vol. 30, no. 2, pp. 198-201, Feb. 1985.

[11] Y.-W. Zhai and Y.-J. Zhao, "Analysis of the inductive iris in rectangular waveguide with the conservation of the complex power technique," *Journal of Xidian University*, vol. 33, no. 4, pp. 630-634, Aug. 2006 (in Chinese).

Feng Lan was born in Sichuan Province, China, in 1977. He received the B.S. degree in electronic engineering and the M.S. degree in optics from University of Electronic Science and Technology of China (UESTC), Chengdu, China, in 2000 and 2007, respectively. He is now a lecturer with School of Physical Electronics, UESTC. His research interests include high power microwave and terahertz sources.

Xi Gao was born in Hunan Province, China, in 1977. He received the M.S. degree in optics from UESTC, Chengdu, China, in 2006. He is currently pursuing Ph.D. degree with School of Physical Electronics, UESTC. His research interests include photonic crystal and terahertz sources.

Zong-Jun Shi was born in Sichuan Province, China, in 1974. She received the M.S. degree in optics from UESTC, Chengdu, China, in 2003. She is currently pursuing Ph.D. degree with School of Physical Electronics, UESTC. Her research interests include high power microwave and terahertz sources.